Hindawi Publishing Corporation
International Journal of Corrosion
Volume 2012, Article ID 368130, 8 pages
doi:10.1155/2012/368130

Research Article

Evaluation of Corrosion Behavior of Galvanized Steel Treated with Conventional Conversion Coatings and a Chromate-Free Organic Inhibitor

Laura A. Hernandez-Alvarado,[1] Luis S. Hernandez,[2] and Sandra L. Rodriguez-Reyna[3]

[1] *Faculty of Chemical Sciences, Universidad Autonoma de San Luis Potosi, Avenida Salvador Nava No. 6, 78290 San Luis Potosi, SLP, Mexico*
[2] *Institute of Metallurgy, Universidad Autonoma de San Luis Potosi, Avenida Sierra Leona No. 550, 78210 San Luis Potosi, SLP, Mexico*
[3] *Faculty of Engineering, Universidad Autonoma de San Luis Potosi, Avenida Salvador Nava No. 8, 78290 San Luis Potosi, SLP, Mexico*

Correspondence should be addressed to Luis S. Hernandez, hersal@uaslp.mx

Received 1 June 2011; Accepted 29 August 2011

Academic Editor: Peter C. Okafor

Conventional weight loss tests and both DC and AC electrochemical techniques were used to study if an organic inhibitor containing an alkanolamine salt of a polycarboxylic acid can substitute toxic coatings as chromating and certain phosphating procedures in the protection of galvanized steel. The electrolyte used was a 0.5 M aerated NaCl solution. All tests gave concordant results, indicating that the chromate-free organic inhibitor does protect galvanized steel in this environment, even though the provided protection was less than that of the chromate conversion coating. It was observed that, after a moderate initial attack, the corrosion rate diminishes due to the appearance and growth of passivating corrosion products layers, mainly constituted by zinc hydroxychloride ($Zn_5(OH)_8CI_2 \cdot H_2O$) and two varieties of zinc hydroxide, among other crystalline compounds.

1. Introduction

Conversion coatings are applied to galvanized steel to improve adhesion of additional protective coatings and for corrosion protection of the zinc coating. Phosphate conversion coatings (PCCs) provide adhesion but do not provide substantial corrosion protection. PCCs provide uniform surface texture and increased surface area, and, when used as a base for paint, they promote good adhesion, increase the resistance of the paint to humidity and water soaking, and eventually increase the corrosion resistance of the painted system [1]. Most galvanized steel used in manufacturing industries (car, household appliances, etc.) is phosphate coated and painted. However, some authors [2] have reported the harmful effects of phosphating, mainly those compositions that contain nickel. Chromate conversion coatings (CCCs) for zinc have been the most widely used, as they enhance bare or painted corrosion resistance, improve the adhesion of paint or other organic finishes, and provide the metallic surface with a decorative finish. CCCs are distinguished by their easy application, their applicability to a wide range of alloys and, in many cases, their ability to improve the galvanized corrosion resistance by virtue of a built-in inhibitor reservoir [3]. Although chromate is an excellent corrosion inhibitor, it is highly toxic; it has carcinogenic effects and must be handled and disposed of with extreme care. Therefore, there are severe restrictions on its use.

Much effort has been devoted to replace chromate chemicals with safe, nontoxic alternatives that are environmentally benign, and many environmental friendly coating systems are under development [4–7]. However, preparation and corrosion behavior of these alternatives is not clear and their practical usage is doubtful. The purpose of this paper is to evaluate the corrosion protection provided by a chromate-free organic inhibitor that is suggested as a nontoxic alternative to chromate and phosphate conversion coatings on galvanized steel. The water-soluble organic inhibitor is based on an alkanolamine salt of a polycarboxylic acid.

Table 1: Some characteristics of the tested coatings.

Coating	Chemical composition	pH	Application method
chromate	200 g potassium dichromate + 6 cc sulphuric acid in 1 L of water	0.8	dipping for 20 sec at room temperature
phosphate	21.0 g acidic zinc phosphate + 1.2 g sodium nitrite + 1.8 g triethanolamine oleate in 1 L of water	5.0	dipping for 600 sec at room temperature
inhibitor 5.0%	water-soluble corrosion inhibitor containing an alkanolamine salt of a polycarboxylic acid	8.0	dipping for 40 sec at 75°C

2. Experimental Procedure

Test specimens of 5 × 10 cm were cut from a mild steel sheet of 1 mm thickness and subsequently submerged in a molten zinc bath to obtain a galvanized coating of 1450 g/m^2, according to ASTM A 90 standard. The specimens were degreased in trichloroethylene, rinsed in distilled water, coated, rinsed again in distilled water, and then dried for seven days prior to submit them to the tests. The chemical composition and other characteristics of the tested coatings are described in Table 1.

The corrosion resistance and paint adhesion characteristics may generally be determined, in addition to the coating weight, by a characteristic color imparted by the chromium compounds formed on the surface of the zinc. After the chromating, the galvanized surface had a dark orange, almost brown, transparent color that made possible to see the zinc grains on the surface. These colored hexavalent chromium conversion coatings are generally considered to give the best overall corrosion protection, as well as poor electrical conductivity and excellent paint adhesion properties [5]. The samples treated with the phosphating solution got a dull black color with granular appearance. Surfaces treated with the inhibitor did not show any visible change at all. The water-soluble corrosion inhibitor contains an alkanolamine salt of a polycarboxylic acid. The tested concentration, application procedures, and elimination of corrosion products of the samples treated with this commercial product were made in strict accordance with the instructions of the manufacturer. For example, a borax solution (35 gL^{-1} at 65°C) was used for elimination of corrosion products. It is claimed that the inhibitor protects galvanized steel by sealing pores and other discontinuities present in the zinc coating. It is also suggested as a replacement of sodium nitride to protect ferrous metallic materials.

The protective effect of these treatments on galvanized steel was studied by immersion tests conducted in a naturally aerated 0.5 M NaCl solution, pH = 6.0, during 134 days and at room temperature. Panels in triplicate were withdrawn from the solution at different periods of time. In all tests, there were included untreated galvanized panels as blanks. The corrosion weight loss parameter was obtained after cleaning the surface of the panels in an acetic acid solution. Other specimens were examined after the same test periods, without stripping the corrosion products, by X-ray diffraction (*XRD*). The *XRD* patterns of the corroded samples were recorded using a diffractometer with a Cu K_α radiation of 1.54056 Å operated at 36 kV/30 mA. The samples were step-scanned in the 2θ range of 5° to 35° with a step size of 0.02 and a time step of 3 s.

In order to perform the electrochemical techniques, glass tubes were attached to the panel surface with a silicone sealer. The tube, that defined an interior exposed area of 10.3 cm^2, was filled with the 0.5 M NaCl solution. The cell contained a graphite electrode as the counter electrode and a saturated calomel electrode (sce) as reference. The open circuit potential (E_{ocp}) and the polarization resistance (Rp) were determined throughout the immersion time. E_{ocp} measurements were carried out previously to Rp. The Rp values were determined by imposing a pulse of ± 10 mV and recording the current system response. In addition, potentiodynamic polarization measurements were carried out at a scan rate of 120 mV/min, from −250 to +500 mV with respect to E_{ocp}. AC impedance measurements were made at the E_{ocp} by using a frequency response analyzer (FRA) operated under microcomputer control. The FRA was connected to the electrochemical cell through a potentiostat. A sinusoidal signal of 10 mV was applied over the frequency range from 100 kHz to 5 mHz. Impedance data were analyzed using a complex nonlinear least-squares program (CNLS). All electrochemical measurements were carried out in triplicate, at room temperature and with no deaeration or stirring of the electrolyte.

3. Results

3.1. Microstructural Characterization of the Coatings. The zinc coating weight of 1450 g/m^2 corresponds to an approximate thickness of 101 μm per side (Figure 1). Figures 2(a) through 2(c) show the backscattered scanning electron micrographs of the untreated and treated galvanized steel samples. The characteristic aspect of microcracking due to dehydration and the shrinkage of the coating during drying are visible in the chromated samples (Figure 2(a)). The surface of the phosphated samples appeared totally covered by a compact layer of small crystals (hopeite) that favors a firm anchorage of organic coatings (Figure 2(b)). Untreated galvanized samples had a very smooth surface and only appeared the limits of the zinc grains, scratches, and white points that correspond to lead particles (Figure 2(c)). The surfaces of the samples treated with the inhibitor (not included here) did not show any difference in comparison with the untreated galvanized ones.

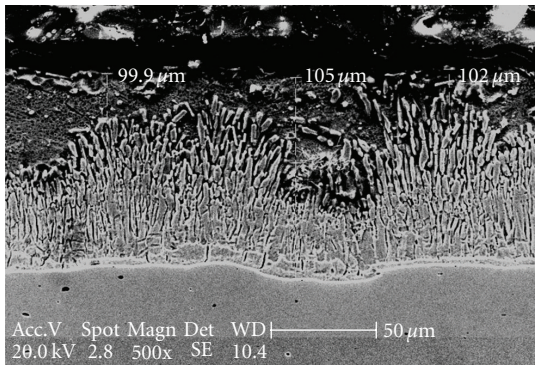

Figure 1: Scanning electron micrograph of the cross section of galvanized steel showing various Zn-Fe alloy layers and the thickness measurements.

3.2. Weight Loss and Electrochemical Measurements. Figure 3 shows the gravimetric results of the considered materials immersed in a 0.5 M NaCl solution up to 134 days. Untreated and treated galvanized steel showed very low corrosion rates, less than 10 mg/cm^2 (~38 μm/y), which are within a range considered as excellent (25–100 μm/y) according to a widely used classification [8]. Furthermore, the corrosion rate values obtained for untreated galvanized steel are approximate to those previously reported by other authors using similar NaCl solutions [9]. It is clearly observed that the inhibitor and the phosphating protected in a moderate way the galvanized steel, although the highest protection is shown by the chromated samples. It is worth mentioning the less steep curve slope of the chromated samples. Regarding the process kinetics, in the early immersion days the four curves show a moderate corrosion rate that diminished as the exposure time elapsed, indicating that corrosion rate was governed by diffusion processes. As the immersion time increased, a white layer of corrosion products appeared over the sample's surfaces, except for the chromate ones; it restricted the access of the solution to the metallic zinc. The chromated samples did not show any visible deterioration.

Regarding the *Rp* variation as function of time (Figure 4), there is an evident difference between the higher values of the chromated samples and the lower values of the other surface conditions. Even at the end of the immersion period, the chromated samples values are still very high compared to those of the other surface conditions (<2500 $\Omega\cdot$cm^2). In general, all samples depicted a very similar performance. In the case of phosphated samples, the *Rp* values were initially low, later they increased with the immersion time, and finally, after 110 days of immersion, they decreased again. This indicates that corrosion exists at the beginning of the immersion and later the *Rp* values increase due to the plugging of the spaces among the hopeite crystals with corrosion products. Afterwards, the movement of the electrolyte during the measurements uncovers the holes again. This behavior was congruent with the evolution of the E_{ocp} values. The *Rp* data were obtained in triplicate; the tendency shown in Figure 4 is representative of the three samples tested for each surface condition.

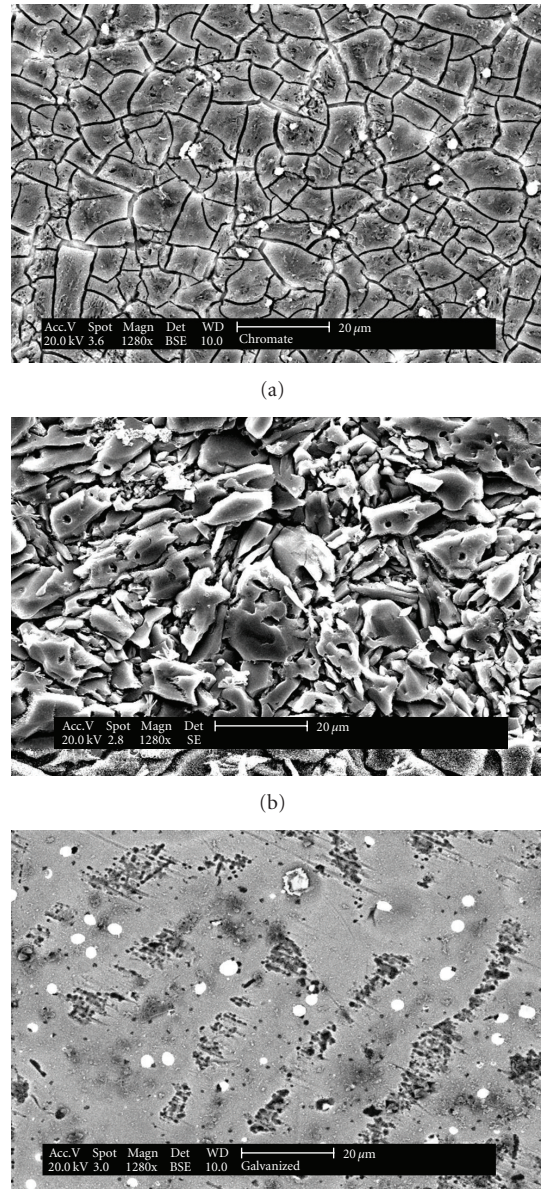

Figure 2: Backscattered scanning electron (BSE) micrographs of the surface conditions of galvanized steel: (a) chromated 1280x, (b) phosphated 1280x, and (c) untreated 1280x.

The E_{ocp} of the four surface conditions exhibited initial values around the known free open circuit potential of uncoated zinc in aerated saline solutions (−900 to −1100 mV$_{sce}$), presenting afterwards two trends (not shown): a permanency (plateau) in this potential range until the 134th day (chromated and inhibitor-treated samples) or a displacement towards nobler potentials as time elapses (phosphated and untreated samples). For these last two surface conditions, the increase of the E_{ocp} was due to the fact that the system evolved towards the uncoated steel E_{ocp} in this environment, as was demonstrated by the presence of abundant rust on the samples at the end of the immersion test.

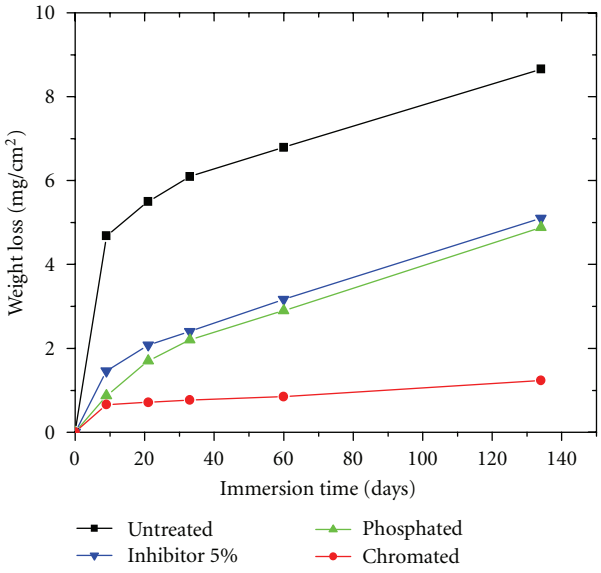

Figure 3: Corrosion performance of galvanized steel with various surface conditions immersed in a 0.5 M NaCl solution during 134 days.

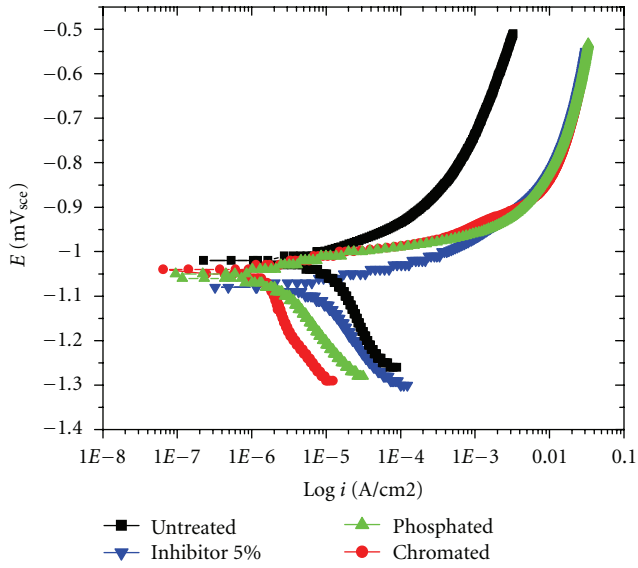

Figure 5: Potentiodynamic polarization curves of galvanized steel with various surface conditions immersed in a 0.5 M NaCl solution during 1 h.

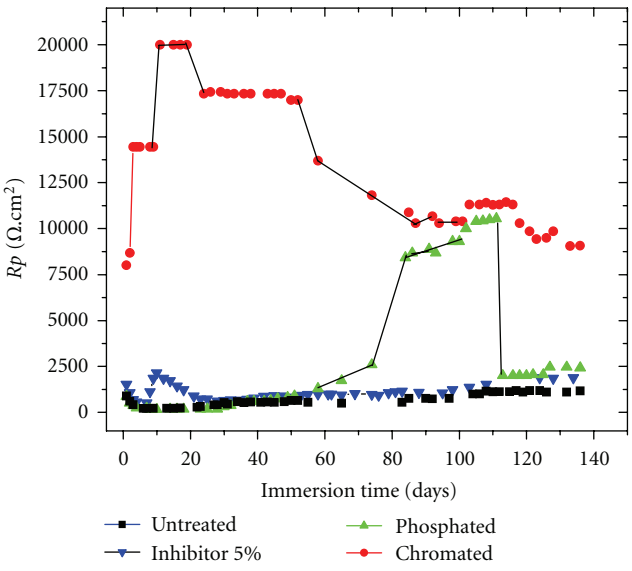

Figure 4: Evolution of *Rp* of galvanized steel with the exposure time with various surface conditions immersed in a 0.5 M NaCl solution.

Figure 5 and Table 2 disclose the polarization curves and electrochemical data of the galvanized steel conditions after immersion in the NaCl solution for 1 h. The curves for each surface condition were obtained at least in duplicate. The polarization scanning was made in the vicinities of the Tafel linear regions in order to calculate numeric values of the corrosion rate. The E_{ocp} of all the samples range from −997 to −1050 mV_{sce}; the nobler values belong to the phosphate samples and the more negative values correspond to the chromate ones.

All the anodic curves are very similar to each other as well as there is a great similarity of all the cathodic curves. The anodic branches show active zinc dissolution and a monotonically increase of current up to very steep slopes, which indicates a diffusion-controlled reaction rate. These branches also show that the different surface treatments increased the anodic dissolution rate with respect to untreated galvanized. This unexpected behavior may be due to the untreated sample's air drying after immersion in the NaCl solution the day previous to the potentiodynamic polarization measurements. It has been reported that air drying after immersion in a 5% NaCl solution drastically reduces the corrosion current of a zinc material. This decrease is attributed to the formation of a more compact corrosion products film as a result of drying [10]. In the cathodic curves, however, there exist a clear reduction in the values of the current density, from the untreated sample to the chromated one, which is exactly of an order of magnitude and that can be confirmed with the i_{corr} values from Table 2, calculated with the potentiostat software. It is worth mentioning the low i_{corr} values of all surface conditions and the fact that anodic slopes values decrease with corrosion rate.

The inhibitive action of chromating is manifested in this decrease of the oxygen rate reduction and has been previously reported by some authors [11, 12]. Moreover, the position of the extreme surface conditions, corresponding to the fastest and the slowest oxygen rate reduction (untreated and chromating, respcting) coincide with the results of weight loss test (Figure 3).

The impedance measurements were taken 1 and 168 h after the electrolyte had made contact with the sample surface. Typical Nyquist impedance diagrams are shown in Figures 6(a) to 6(c) for the phosphated, chromated and untreated galvanized samples after 1 h, respectively, whereas Figure 6(d) depicted the diagram for an untreated sample after 168 h. In these figures, the experimental diagrams are

Table 2: Electrochemical data of the tested materials after immersion in 0.5 M NaCl for 1 h.

Condition	β_a (mV/decade)	β_c (mV/decade)	i_{corr} (μA/cm^2)	E_{oc}/E_{corr} (mV$_{sce}$)	Corrosion rate (mpy)	Ch Sq
Untreated	88	367	11.9	−1033/−1050	7.0	$3.67e^{-6}$
Inhibitor 5%	44	224	6.9	−1046/−1080	4.0	$3.75e^{-6}$
Phosphated	52	201	1.8	−1010/−1020	1.0	$4.07e^{-6}$
Chromated	35	278	1.1	−1050/−1040	0.7	$4.09e^{-6}$

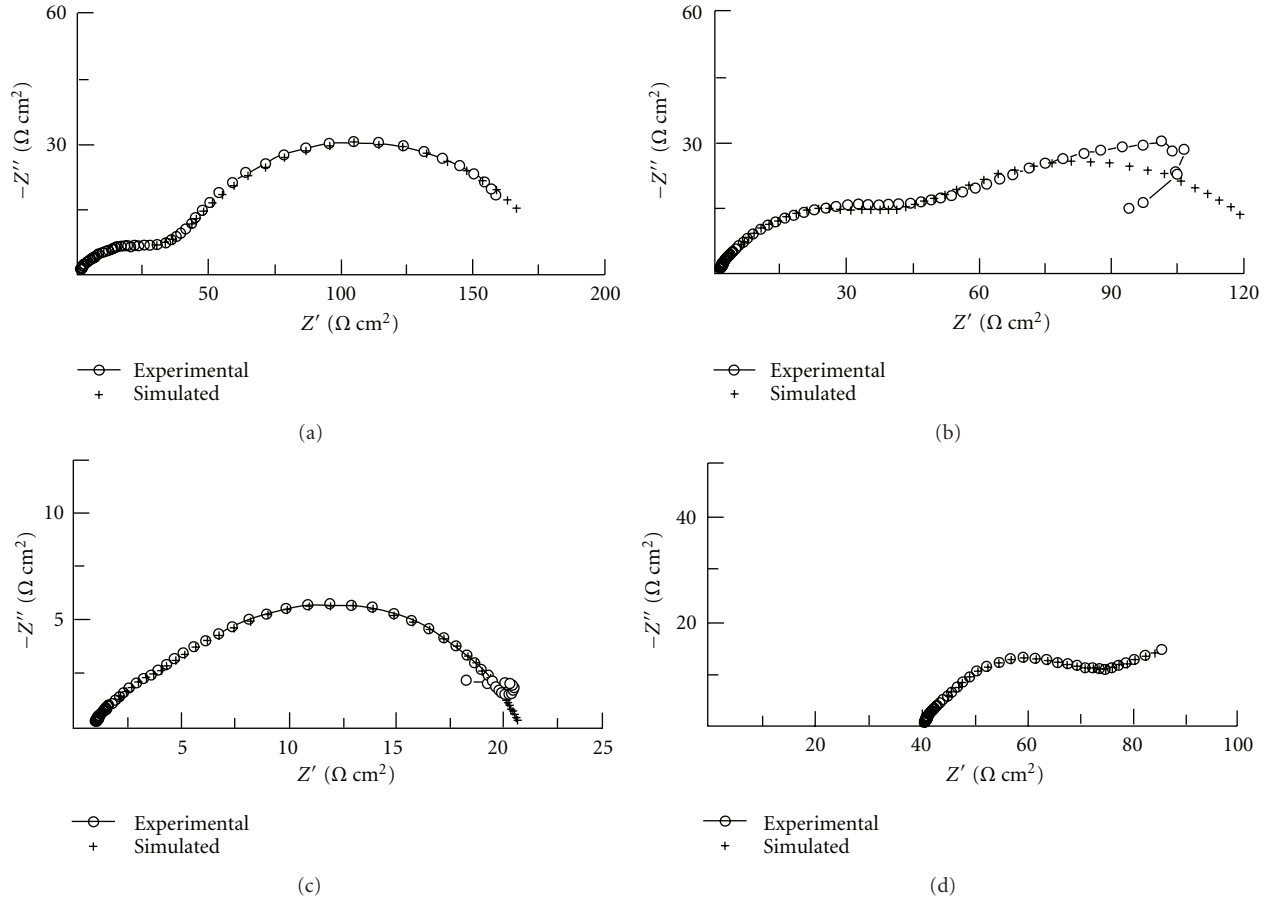

Figure 6: Experimental and simulated Nyquist impedance diagrams of galvanized steel with various surface treatments immersed in a 0.5 M NaCl solution during 1 h (a) phosphated, (b) chromated, (c) untreated, and (d) untreated immersed during 168 h.

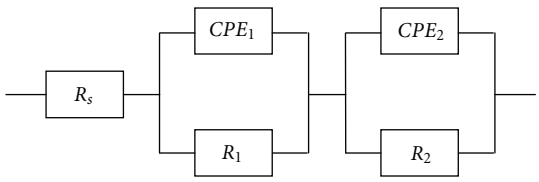

Figure 7: Equivalent electric circuit model used to fit the impedance data for treated and untreated galvanized samples.

overlapped with the simulation ones; these were obtained using a nonlinear least-squares fitting analysis procedure with the equivalent electric circuit model shown in the Figure 7. This circuit showed the best adjustment to the coated samples impedance data: R_s is the resistance of the electrolyte, CPE_1 is a constant-phase element related to the capacitance of the coating, R_1 is the coating pore resistance due to electrolyte penetration, CP_2 is a constant-phase element related to the double-layer capacitance and diffusion processes [13], and R_2 is the charge transfer resistance. CPE_1 and R_1 are associated with the zinc coating on steel in the untreated galvanized samples. The diagrams have different shapes and values at the low frequency limit. The phosphated and chromated samples exhibited larger values than the untreated ones. The samples treated with the organic inhibitor showed impedance diagrams very similar to those of untreated samples and are not shown. In general, the impedances measured after 1 h decreased after 168 h of contact with the electrolyte, except for the chromated condition.

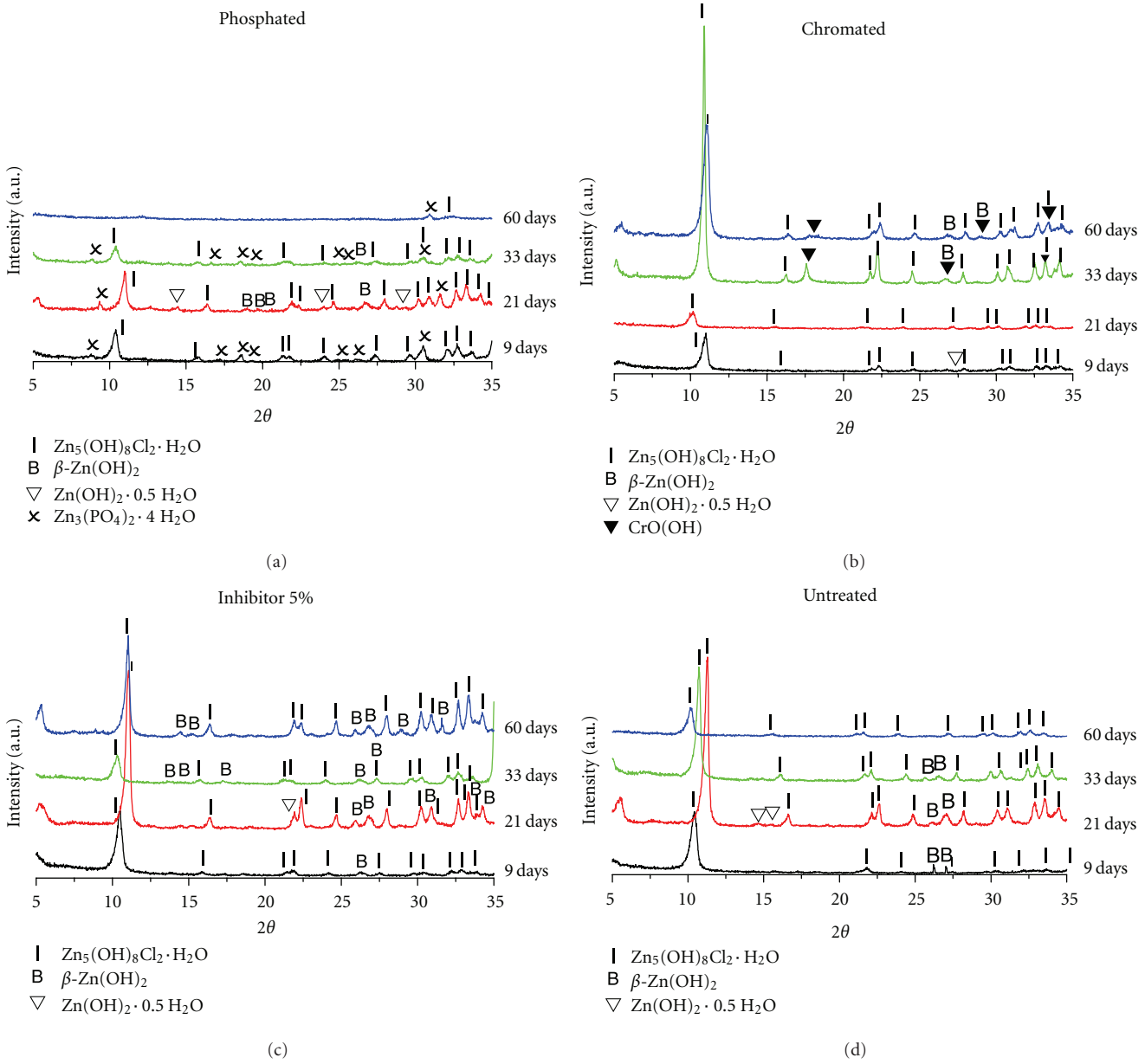

Figure 8: XRD spectra of corrosion products obtained after different immersion periods.

According to the interpretation of this type of complex plane plots, the samples after one hour of immersion showed two frequency-dependent components: an initial high frequency semicircle, less defined for the untreated sample (Figure 6(c)), and a second component clearly defined in the low frequency range. This component is a greater second semicircle for phosphated and untreated surfaces and seemingly a diffusion tail (Warburg impedance) for chromate sample. It is generally accepted that both second components (semicircle or diffusion tail) appear as a consequence of a diffusion controlled corrosion process, related mainly with the oxygen reduction. An equivalent electric circuit for plots like these assumes that the diffusion process is much slower than the charge-transfer reaction and that diffusion is rate-controlling [14].

For untreated galvanized steel samples, the size of the second semicircle decreases as the immersion time increases and a capacitive branch appears in the low frequency range. Concerning the low frequency end observed in Figures 6(b) and 6(c), this behavior has been attributed, namely, to a potential drift [15]; this "tail back" is due probably to the effect of changing potential on the impedance response.

3.3. XRD of Corrosion Products and Salt Spray Test. Figure 8 presents the *XRD* spectra of corrosion products, the chemical composition of the detected compounds and the periods when they appeared. In all the samples, was identified zinc hydroxychloride ($Zn_5(OH)_8Cl_2 \cdot H_2O$), known as Simonkolleite, and in most of the samples at least two varieties of $Zn(OH)_2$ were detected.

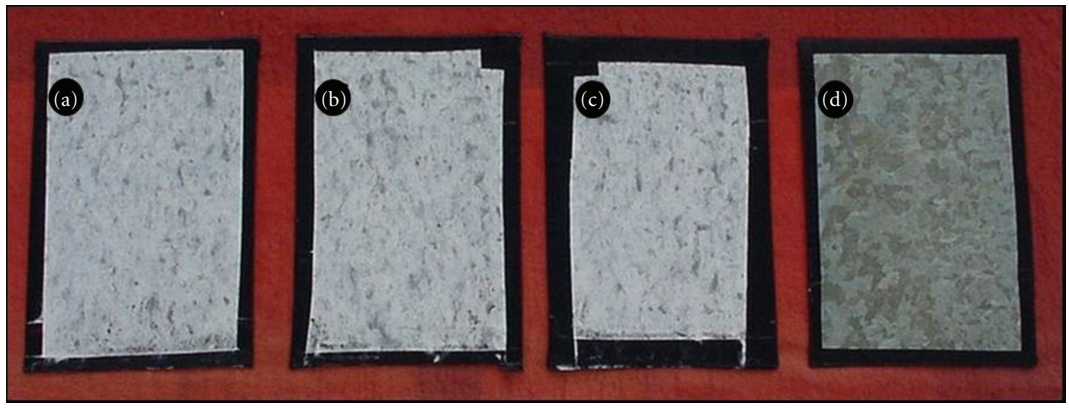

Figure 9: Aspects of the surface conditions of the galvanized steel after 168 h in the saline fog chamber: (a) untreated, (b) inhibitor 5%, (c) phosphated, (d) chromated. The whitish aspect of the first three samples is due to the zinc corrosion products.

Hopeite ($Zn_3(PO_4)_2 \cdot 4H_2O$) was detected in all the phosphated samples analyzed. Bracewellite (CrO(OH)) appeared only after 33 and 60 days of immersion on the surfaces of the chromated samples. It is a compound supposed to exist in accelerated chromium chromate coatings [16]. The peaks displacement in de *XRD* spectra are due to an inadequate sample alignment.

The presence of CrO(OH) after 33 days of immersion is due to the dissolution of the coating's amorphous hexavalent compounds, remaining an insoluble trivalent chromium compounds layer. Composition depth profiles indicate that the hexavalent chromium compounds exist predominantly in the outer portion of the coating [16, 17]. The ß-$Zn(OH)_2$ seems also to be present only in two specific periods, since the composition of zinc corrosion products in chloride solutions depends on the exposure time, so the hydroxides exists just temporarily, becoming hydroxychlorides as immersion time elapses, as it will be explained later.

Samples of the different surface conditions of galvanized steel were submitted to a salt spray test applying the ASTM B 117 method, which was carried out in triplicate. The appearance of the samples was evaluated at different time intervals with a maximum of 168 hours. By then all samples, except the chromated ones, were totally covered by white corrosion products and also presented incipient red corrosion. The chromated samples, on the other hand, appeared lustrous and only in one of them the dark orange color had disappeared (Figure 9).

4. Discussion

In the immersion test, the high initial corrosion rates, except for the chromated samples, are a consequence of the anodic dissolution of treated or untreated galvanized steel before forming the corrosion products. As long as immersion time increased, a white layer of corrosion products appeared over all samples' surfaces, except on the chromated ones, and the high initial values of corrosion rate decreased. These white films, which resulted in being protector, got thicker with time, causing the corrosion rate to decrease even more. Regarding the chromate samples, it has been reported that, as far as the surface preserves its dark orange, almost brown aspect, Cr^{6+} ions have not been leached and the coating is still protecting the zinc substrate [18].

With regard to this white corrosion products layer, Feitknecht [19] previously reported the presence of zinc hydroxychloride and zinc hydroxide in immersion tests in a NaCl solution of the same concentration as that used in this study, and they also appear in the reaction sequence for zinc exposed in natural marine atmospheres [20]:

$$\mathrm{Zn} \longrightarrow \mathrm{Zn(OH)_2} \longrightarrow \mathrm{ZnCl_2 \cdot nZn(OH)_2} \qquad (1)$$

with $n = 4$ for Simonkolleite. Several explanations for the apparent corrosion-inhibiting nature of Simonkolleite have been proposed, trying to justify the fact that the higher the amount of Simonkolleite in the corrosion products, the higher the resistance to corrosion [21]: (1) it has been considered that it is a more compact corrosion product than ZnO because the *c* axis of the hexagonal close-packed structure of Simonkolleite is parallel to the film corrosion products growth direction, (2) it probably decreases the oxygen reduction rate on itself, (3) that is due to its low solubility product (8.2×10^{-76}). On the other hand, crystalline and amorphous varieties of $Zn(OH)_2$ have been detected using cyclic voltammetry in chloride containing electrolytes [22]. It has been reported that the amorphous variety has a higher solubility product and is metastable.

The impedance diagrams, whose low frequency semicircle or tail may indicate a finite thickness layer diffusion process, related mainly with the oxygen reduction, confirmed that the corrosive process is governed by diffusion, as it is also indicated by the weight loss and *DRX* results. According to Barranco et al. [23], it is likely that a complex mass transport mechanism intervenes in the system formed by the corrosive medium/corrosion products/metal, both in the liquid phase and through the corrosion products layer that coats the metallic surface.

Finally, the *Rp* values of the samples, except for the chromated ones, were too low to ensure an acceptable protection. These values were inferior to 2500 $\Omega \cdot cm^2$ during

the test period and did not increase at the end of the test in spite of the rust presence in the phosphated and untreated galvanized samples.

5. Conclusions

The organic inhibitor does protect galvanized steel in a 0.5 M NaCl solution, even though the higher protection was provided by the chromate conversion coating. So, if the organic inhibitor will substitute chromating, other considerations should be kept in mind. The quiescent nature of the electrolyte definitely contributed to this protection, because it allowed the corrosion products layers to remain on the surface during the immersion time.

The corrosion rate of galvanized steel, with the different surface conditions, decreased with time. This decrease was associated with the formation and growth of adherent, white corrosion products layers on the metallic surface, mainly composed of zinc hydroxychloride and zinc hydroxide. These layers limited the dissolved oxygen access to the treated or untreated surfaces of galvanized steel, causing the processes in the surface to be controlled by diffusion.

Regarding the chromate conversion coating, even though there was not a great amount of white corrosion products films, they were detected in XRD spectra. The higher protection provided by the this conversion coating to galvanized steel was mainly due to its own nature and it was confirmed by the polarization resistance results, and by the notable inhibition of the oxygen reduction reaction observed in the cathodic potentiodynamic polarization branches.

References

[1] X. G. Zhang, *Corrosion and Electrochemistry of Zinc*, Plenum Press, New York, NY, USA, 1996.

[2] J. F. McIntyre and R. J. Brent, "Tendencies of the pretreatment technology in next millennium," *Pinturas y Acabados Industriales*, vol. 42, no. 261, pp. 36–44, 2000.

[3] R. G. Buchheit, S. B. Mamidipally, P. Schmutz, and H. Guan, "Active corrosion protection in Ce-modified hydrotalcite conversion coatings," *Corrosion*, vol. 58, no. 1, pp. 3–14, 2002.

[4] S. A. Furman, "Novel coating technology replaces chromate in zinc galvanizing process," *Materials Performance*, vol. 49, no. 1, pp. 10–12, 2010.

[5] J. W. Bibber, "Chromium-free conversion coatings for zinc and its alloys," *Journal of Applied Surface Finishing*, vol. 2, no. 4, pp. 273–275, 2009.

[6] T. Peng and R. Man, "Rare earth and silane as chromate replacers for corrosion protection on galvanized steel," *Journal of Rare Earths*, vol. 27, no. 1, pp. 159–163, 2009.

[7] A. D. King and J. R. Scully, "Sacrificial anode-based galvanic and barrier corrosion protection of 2024-T351 by a MG-rich primer and development of test methods for remaining life assessment," *Corrosion*, vol. 67, no. 5, Article ID 055004, 22 pages, 2010.

[8] M. G. Fontana, *Corrosion Engineering*, McGraw-Hill, Singapore, 3rd edition, 2008.

[9] M. Toga, P. Moyo, and D. J. Simbi, "Corrosion of galvanized steel in simulated mine water environments," in *Proceedings 15th International Corrosion Congress*, paper 231, 9 pages, Granada, Spain, 2002.

[10] M. Sagiyama, A. Hiraya, and T. Watanabe, "Electrochemical behavior of electrodeposited zinc-iron alloys in 5%NaCl solution," *Journal of the Iron and Steel Institute of Japan*, vol. 77, no. 2, pp. 244–250, 1991.

[11] R. L. Zeller and R. F. Savinell, "Interpretation of A.C. impedance response of chromated electrogalvanized steel," *Corrosion Science*, vol. 26, no. 5, pp. 389–399, 1986.

[12] A. A. O. Magalhaes, I. C. P. Margarit, and O. R. Mattos, "Electrochemical characterization of chromate coatings on galvanized stell," in *Proceedings of the International Symposium on Electrochemical Impedance Spectroscopy (EIS '98)*, pp. 239–241, Rio de Janeiro, Brazil, 1998.

[13] F. Deflorian, V. B. Miskovic-Stankovic, P. L. Bonora, and L. Fedrizzi, "Degradation of epoxy coatings on phosphatized zinc-electroplated steel," *Corrosion*, vol. 50, no. 6, pp. 438–446, 1994.

[14] C. Lin, T. Nguyen, and M. E. McKnight, "Relation between AC impedance data and degradation of coated steel. 1. Effects of surface roughness and contamination on the corrosion behavior of epoxy-coated steel," *Progress in Organic Coatings*, vol. 20, no. 2, pp. 169–186, 1992.

[15] L. M. Callow and J. D. Scantlebury, "Electrochemical impedance on coated metal electrodes. Part1: Polarization effects," *JOCCA*, vol. 64, no. 2, pp. 83–87, 1981.

[16] R. G. Buchheit and A. E. Hughes, "Chromate and chromate-free conversion coatings," in *Corrosion: Fundamentals, Testing and Protection*, vol. 13A of *ASM Handbook*, pp. 720–35, ASM International, Materials Park, Ohio, USA, 2003.

[17] I. Suzuki, *Corrosion-Resistant Coatings Technology*, Marcel Dekker, New York, NY, USA, 1989.

[18] W. Zhang and R. G. Buchheit, "Effect of ambient aging on inhibition of oxygen reduction by chromate conversion coatings," *Corrosion*, vol. 59, no. 4, pp. 356–362, 2003.

[19] W. Feitknecht, "Studies on the influence of chemical factors on the corrosion of metals," *Chemistry and Industry*, vol. 36, pp. 1101–1109, 1959.

[20] V. Kucera and E. Mattsson, "Atmospheric corrosion," in *Corrosion Mechanisms*, F. Mansfeld, Ed., pp. 211–284, Marcel Dekker, New York, NY, USA, 1987.

[21] X. G. Zhang, *Corrosion and Electrochemistry of Zinc*, Plenum Press, New York, NY, USA, 1996.

[22] C. M. Rangel and L. F. Cruz, "Zinc dissolution in lisbon tap water," *Corrosion Science*, vol. 33, no. 9, pp. 1479–1493, 1992.

[23] V. Barranco, S. Feliu Jr., and S. Feliu, "EIS study of the corrosion behaviour of zinc-based coatings on steel in quiescent 3% NaCl solution. Part 1: directly exposed coatings," *Corrosion Science*, vol. 46, no. 9, pp. 2203–2220, 2004.